Tuning Fermi-Surface Properties through Quantum Confinement in Metallic Metalattices: New Metals from Old Atoms

J. E. Han and Vincent H. Crespi*

Department of Physics and the Center for Materials Physics, The Pennsylvania State University, 104 Davey Lab, University Park, Pennsylvania 16802-6300

(Received 4 August 2000)

We describe a new class of nanoscale structured metals wherein the effects of quantum confinement are combined with dispersive metallic electronic states to induce modifications to the fundamental low-energy microscopic properties of a three-dimensional metal: the density of states, the distribution of Fermi velocities, and the collective electronic response.

DOI: 10.1103/PhysRevLett.86.696 PACS numbers: 73.22.–f, 73.21.–b, 73.63.–b, 78.67.–n

Quantum confinement in zero-, one-, and two-dimensional semiconductor and metallic nanostructures has enabled an enormous range of condensed matter physics and material science over the past two decades. The basic electronic property of a semiconductor, the band gap, can be tuned continuously via quantum confinement in nanoparticles. In contrast, the fundamental defining property of a metallic Fermi liquid, the Fermi surface, is lost in a quantum dot, since confinement creates nondispersive electronic states. Although dispersive low-energy states can be recovered in low-dimensional metals such as nanowires and two-dimensional electron gases, the degrees of freedom in the confined and nonconfined directions typically decouple, so that the direct effects of quantum confinement are restricted to the confined dimension(s) and often have relatively minor effects on the single-particle dispersion along the nonconfined direction. Here we propose a new class of materials that combines quantum confinement with a continuum of three-dimensional delocalized, dispersive electronic states through the infiltration of metal atoms into a three-dimensional colloidal lattice (see Fig. 1). The resulting system has a hierarchy of periodicities: the underlying atomic structure resides within the larger-scale periodic colloid, hence the term "metalattice." This metalattice exploits finite size effects to tune the fundamental low energy (i.e., near Fermi energy) properties of the metallic state.

Colloidal crystals on the scale of optical wavelengths have been used as scaffolds for the infiltration of dielectrics into the ordered pore structure to create photonic materials. Here we consider a new regime by extending these colloids to the 1–10 nanometer scale and studying infiltration with metals. Electrochemical deposition, pressure-induced filling, and iterative chemical reduction of metallic salts are all being exploited to infiltrate colloidal systems with metal atoms. Such systems are just starting to be produced at nanometer length scales: for example, Pt has recently been infiltrated into colloidal crystals composed of 30 nm silica spheres with prospects for extension to smaller sizes [1]. As yet, no theoretical treatment exists for the electronic properties of these ordered nanoscale infiltrant metals. We demonstrate here that these three-dimensional metallic metalattices induce several new physical effects such as the following: (1) Fermi velocity *shadowing,* wherein the ordered interconnecting necks within the structure induce pronounced modifications into the distribution of Fermi velocities; (2) bifurcation of the electronic states into two intimately interspersed yet distinct ladders of strongly and weakly dispersive states, a separation which affects the optical response, transport, and density of states at the Fermi level; and (3) the potential for a rich interaction of the large-scale (i.e., colloidal) structural order parameter with other order parameters of the metallic component (e.g., characteristic superconducting length scales, etc.).

Each of the effects discussed above applies across a wide class of metals. For the purposes of an initial case study, we focus on an archetypal example: a face-centered-cubic (fcc) lattice of insulating colloidal spheres, a typical closed packed structure, which is infiltrated with aluminum (see Fig. 1). Although aluminum is not the easiest metal to

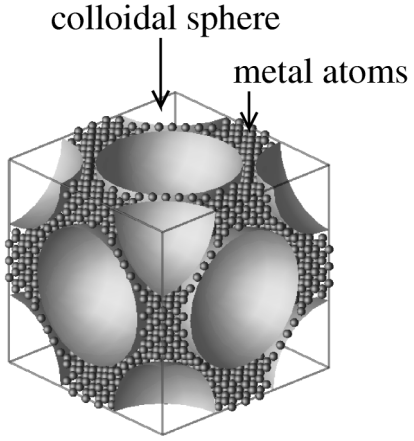

FIG. 1. A face-centered-cubic lattice of insulating colloidal spheres which has been infiltrated with (much smaller) metal atoms. The colloidal spheres are shown as nearly touching with a volume ratio of $V_{\mathrm{Al}}/V_{\mathrm{total}} = 27\%$; they contain a $12 \times 12 \times 12$ three-dimensional hierarchical superlattice, or metalattice, of metal atoms. The cross section of a neck (not easily visible above) contains about 10 metal atoms.

 0031-9007/01/86(4)/696(4)$15.00

infiltrate experimentally, its simple electronic structure and theoretical tractability make it a useful "canonical metal" [2] that can clearly elucidate the generic features of the new physics. We assume that the aluminum atoms also crystallize in the fcc structure inside of the interstitial regions of the lattice, similar to the structures of Al clusters [3]. For computational convenience, we have chosen the colloidal and Al lattices to be in alignment (but note that our main results arise from the large-scale geometry of three-dimensional confinement, not the detailed atomic-level structure of metal). In this initial investigation we do not explicitly treat surface reconstructions, which are in any case much less extensive in metallic systems than in e.g., covalently bonded semiconductors. We describe disorder through both a phenomenological broadening and also a random variation in the on-site energies. Later we discuss the differential sensitivity of various phenomena to disorder.

We compute the electronic structure with an empirical s, p, d-orbital tight-binding method whose parameters are obtained by fitting to the bulk band structures of Würde *et al.* [4]. We construct the systems of study by removing, from the bulk, Al atoms that fall within the colloidal particles. The resulting aluminum structure then comprises octahedral and tetrahedral Al islands interconnected by thin metallic necks. The volume ratio of aluminum, x ($\equiv V_{\mathrm{Al}}/V_{\mathrm{tot}}$), is roughly $1 - \frac{16\pi}{3}(R/L)^3$, with R the radius of colloidal spheres and L the lattice constant of metalattice cubic unit cell. In the physically relevant limit of touching colloidal spheres, $x \approx 0.26$ with $R = L/2\sqrt{2}$. For computational reasons, we restrict the study to systems up to the $12 \times 12 \times 12$ metalattice, although many of the effects discussed will persist up to larger sizes.

Remarkably, instead of narrowing uniformly across all bands, the electronic structure forms sets of very weakly dispersive states which are interconnected by more strongly dispersive bands. Figure 2 shows the electronic structure around the Fermi energy for an $L = 3.6$ nm colloidal lattice containing a $9 \times 9 \times 9$ Al metalattice at $x = 0.27$. The weakly dispersive states occupying regions around, e.g., $-0.05 \leftrightarrow 0.00$ and $0.08 \leftrightarrow 0.1$ eV are interconnected by bands of substantially more dispersive states. This classification is also seen in real space: the weakly dispersive states predominately occupy the interiors of the tetrahedral and octahedral islands, whereas the dispersive states occupy the surfaces and interconnecting necks. The weakly dispersive states evolve smoothly into the localized states of an isolated quantum dot as the lattice connectivity is reduced through, e.g., expanding the colloidal spheres (theoretically) until they interpenetrate and cut off the necks. Since the islands contain many more atoms than the necks, most electrons propagating in an island will reflect from the necks and thereby acquire only weak dispersion. The weakly dispersive states (which are likely to localize under disorder) then form a set of broadened levels with a granularity which is affected by the size of the islands and the point symmetry of the metalattice. In contrast, the more strongly dispersive states form a new class of confined electronic wave functions which do not have an analog in quantum dots.

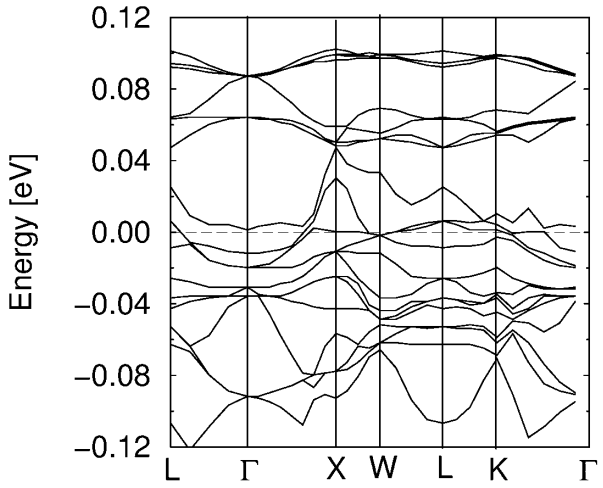

FIG. 2. Band structure along symmetry directions for a $9 \times 9 \times 9$ metalattice with touching colloidal spheres. Localized states over energies, e.g., $0.0 \leftrightarrow -0.05$ and $0.08 \leftrightarrow 0.1$ eV, come from interior sites in Al clusters. Delocalized states interconnecting localized states have significant density on surface and neck sites. The Fermi energy is set to 0 eV.

This granularity in the weakly dispersive manifold produces strong modulations in the density of states at the Fermi level, even under the influence of a moderate ($\sim$0.2 eV) phenomenological disorder-induced broadening [5]. The main plot in Fig. 3 illustrates this effect by showing the evolution of the density of states as colloidal spheres of variable size but fixed spacing is introduced into the metalattice. (Note that the intermediate values of x are not experimentally accessible, since the spheres are

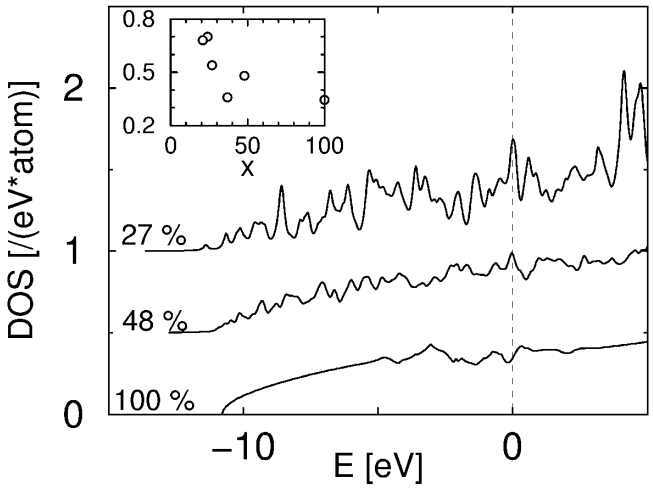

FIG. 3. Density of states for varying colloidal radii for a $9 \times 9 \times 9$ metalattice. The main plot shows the emerging peaks with decreasing volume ratio x ($\equiv V_{\mathrm{Al}}/V_{\mathrm{tot}}$). With touching colloidal spheres ($x = 27\%$), the DOS peaks due to nearly localized states. The DOS at the Fermi energy ($E_F = 0$) tends to increase with decreasing x (inset).

not touching; instead they provide a well-defined means to understand the effects of variable quantum confinement at a fixed colloidal lattice constant.) The calculation covers 89 **k** points in the irreducible first Brillouin zone with a Lorentzian broadening of 0.2 eV (full width at half maximum) to describe disorder and thermal smearing. The familiar nearly free electronlike density of states of bulk aluminum (bottom curve) is only slightly changed by the introduction of periodic voids in the Al lattice at a volume density of $1 - x = 0.52$. However, when the colloidal spheres touch at $x = 0.27$, the density of states changes significantly and displays peaks (arising from the weakly dispersive states) around E_F. Statistically, the Fermi energy tends to fall near such a peak because such states represent the majority of available states (i.e., the necks compose only a small fraction of the total atoms) and a random filling of the band structure will tend to locate the Fermi level in a peak (we neglect the effects of structural relaxation here). The inset shows the variation in the Fermi-level density of states as the volume filling fraction is decreased from the bulk lattice ($x = 1.0$) to the case of touching colloidal spheres ($x = 0.27$). As expected, the density of states shows a general trend towards higher values at smaller volume fraction. The effect, even under significant ($\sim$0.2 eV) disorder broadening, can be dramatic: at $x = 0.27$ the density of states at the Fermi level is more than twice the bulk value. The specific width of disorder broadening will depend on the detailed characteristics of any given sample; regardless, it is surprising and encouraging that the granularity can survive a broadening which is many times the level spacing expected for quantum dots of similar size.

The bifurcation of the bulk electronic structure into the weakly and strongly dispersive states of the metalattice also has pronounced consequences for the collective electronic response. The plasma frequency ω_p can be calculated from the sum rule for the optical conductivity $\sigma(\omega)$:

$$\int_0^\infty \sigma(\omega)\, d\omega = \omega_p^2/8\,, \tag{1}$$

where $\omega_p^2 = 4\pi n e^2/m^*$ with n the charge carrier density in a naive kinetic model. For the bulk lattice, we obtain $w_p = 16.3$ eV, in good agreement with experiment [6]. The infiltrated Al metalattice has a much reduced plasma frequency: 7.2 and 6.6 eV for $6 \times 6 \times 6$ and $9 \times 9 \times 9$ metalattices, respectively. The ratio of effective charge carriers, $n_{\text{metalat}}/n_{\text{bulk}} = \omega_{p,\text{metalat}}^2/\omega_{p,\text{bulk}}^2 = 0.19$ and 0.16, respectively, cannot be ascribed solely to the reduced volume fractions of $x = 0.35$ and 0.27. Instead, the large reduction demonstrates that roughly half of the charge carriers in the infiltrated metal effectively do not participate significantly in this aspect of the collective optical response due to a strongly enhanced effective mass. Since the two classes of electronic states are intimately interspersed in energy, they are unlikely to decouple into distinct plasmons, as would be the case for, e.g., σ and π plasmons in carbon.

The strongly anisotropic lattice connectivity within the infiltrated colloid also causes qualitative changes to the pattern of Fermi velocities around the Fermi surface of the metal infiltrant. Figure 4(a) shows the Fermi velocities for bulk Al projected onto a unit sphere. We have weighted each Fermi velocity vector with its magnitude and then smeared slightly to obtain a continuous distribution. The Fermi velocity of bulk Al is largest (dark region) along the body-diagonal direction. In contrast, as shown in Fig. 4(b), the Fermi velocities in the infiltrated $9 \times 9 \times 9$ Al metalattice concentrate along $(1, 0, 0)$ directions. The remarkable inversion, i.e., *shadowing,* in the distribution of Fermi velocities between the bulk and colloidal lattices arises because the electron transport in the infiltrated metal is greatly hindered by the large unpenetrable colloidal spheres which suppress the Fermi velocity strongly along the body-diagonal directions. The nondispersive states are effectively filtered out from electron transport and the dispersive states dominate the Fermi velocity distribution. Since the dispersive states predominately occupy the surface and necks, the symmetry of the Fermi velocity distribution is primarily determined by the overall connectivity of the metal surface, although its details are sensitive to the atomic-scale structure of the surface. We expect these qualitative features to hold regardless of lattice alignments or the lattice structure of metal infiltrant so long as the size of the colloidal lattice is smaller than relevant length scales in the metal (e.g., the mean free path).

Interesting phenomena also appear in the optical conductivity, even within a simplified isotropic phenomenological model of the scattering (see Fig. 5). For simplicity, we choose a uniform scattering rate $1/\tau = 0.1$ eV; this choice isolates the effects of the modified Fermi-level states from those due to possible confinement/surface-induced modulations in scattering processes [7]. (A more complete treatment of scattering might reveal new structure in the frequency dependent conductivity as, e.g., v_F/ω approaches the colloidal lattice constant.)

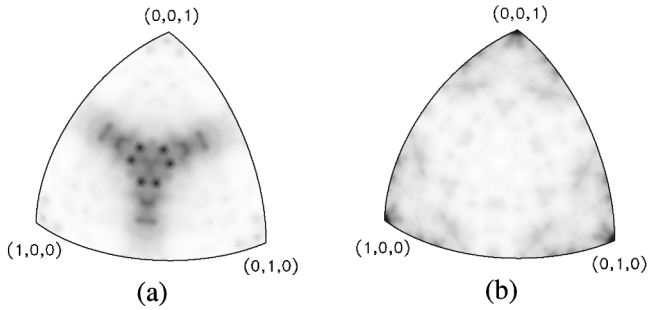

FIG. 4. (a) Bulk aluminum Fermi velocities projected onto a unit sphere with the intensity proportional to the magnitude of v_F. The Fermi velocity is largest along the body diagonal direction. (b) A similar plot for a $9 \times 9 \times 9$ metalattice with touching colloidal spheres: the shadow of (a). Dispersive bands contribute to the Fermi velocities along $(1, 0, 0)$ directions. The Fermi velocity along $(0, 0, 0)$ is strongly suppressed due to intervening colloidal particles.

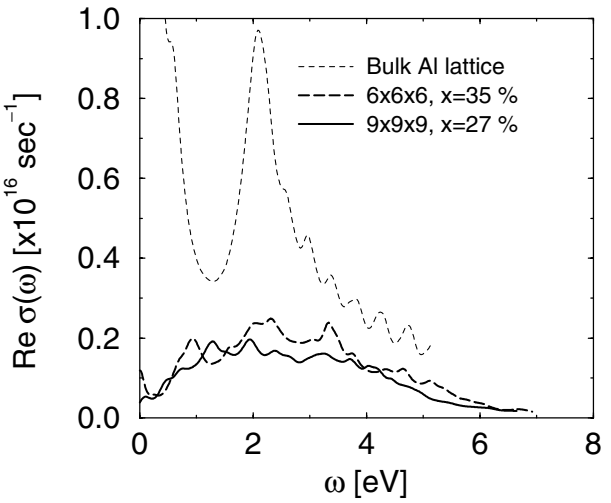

FIG. 5. Optical conductivity for a bulk Al lattice and metalattice with scattering rate $\hbar/\tau = 0.1$ eV. In the colloidal lattice the intraband contribution (i.e., the Drude part) is strongly reduced due to nondispersive states. The oscillating tail for bulk Al is an artifact of the finite **k** mesh.

For the bulk lattice, the intraband Drude peak dominates, while the first two interband transitions (the first one is buried under the Drude peak) give additional structure which is also in good agreement with experiment [2,8]. Despite the large number of states, the weakly dispersive states contribute only weakly to the optical conductivity due to their small Fermi velocity. Transitions between the dispersive states dominate the optical conductivity.

These new phenomena in the bulk-confined ordered metallic state have variable sensitivity to disorder, including atomic-scale displacements, variations in colloidal particle size, and grain boundaries within the metal or colloidal template. The detailed structure of particular bands as presented here is the feature most sensitive to disorder, as fluctuations on the order of the (folded) bandwidth are likely inescapable in the real systems. However, the coarsened separation of electronic states into weakly and strongly dispersive states persists over the entire multi-eV bulk (i.e., unfolded) bandwidth and the density of state modulations can survive a broadening greatly in excess of the band spacing. As this classification relates to the differential occupation of island and neck sites, it is more robust than the details of any single specific band. Similarly, the shadowing of the Fermi velocity distribution arises directly from the anisotropic metalattice connectivity, which is also relatively robust under atomic-scale disorder. Finite grain size will smear the Fermi surface, but the Fermi velocity symmetry and weakly/strongly dispersive character of the states exists over the entire Brillouin zone. Note that, as a function of colloidal lattice period, different properties approach the bulk limit at different sizes: the long-range spatial coherence over a single band state is destroyed by very weak disorder in larger-scale systems, whereas the density of states fluctuations can survive to significantly larger sizes (or similarly, larger disorder smearings), and the shadowing in the angular distribution of the electronic dispersion can also persist to larger colloidal-lattice periodicities.

Particularly intriguing properties emerge as the lattice constant of the infiltrant (and the associated structural order parameter) approaches other characteristic length scales in the metal. For example, at larger colloidal sizes (several hundred angstroms and higher) where many of the atomic-scale electronic modulations described above will begin to wash out, the collodial lattice structural order parameter will begin to interact richly with, e.g., characteristic superconducting length scales such as the penetration depth, with potentially fascinating consequences for the magnetic response of metalattice type I or type II superconductors. In addition, across a range of length scales the electron screening and transport response will be sensitive to the physical and chemical configuration of the surface and interstitial spaces. Since the original colloidal lattice can be etched away, this newly liberated interstitial space within the metallic metalattice is available for surface functionalization or second infiltration, both of which could be reversible in certain cases (i.e., for a fluid infiltrant). For example, a backfilling infiltration with a dielectric medium into an open metallic metalattice would modulate the electron-electron interaction, particularly across the void regions. The single-particle band structure results given here provide a base of understanding towards further study of this fascinating class of materials.

We thank P. Eklund and T. Mallouk for helpful discussions. We gratefully acknowledge the David and Lucile Packard Foundation, the National Science Foundation through Grant No. DMR-9876232, the Materials Research Science and Engineering Center *Collective Phenomena in Restricted Geometries,* and the National Partnership for Advanced Computational Infrastructure and the Pittsburgh Supercomputing Center for computational support.

*Electronic address: vhc2@psu.edu

[1] G. L. Egan, J.-S. Yu, C. H. Kim, S. J. Lee, R. E. Schaak, and T. E. Mallouk, Adv. Mater. **12**, 1040 (2000).
[2] N. W. Ashcroft and K. Sturm, Phys. Rev. B **3**, 1898 (1971).
[3] B. K. Rao and P. Jena, J. Chem. Phys. **111**, 1890 (1999).
[4] K. Würde, A. Mazur, and J. Pollmann, Phys. Status Solidi **179**, 399 (1993).
[5] Disorder in the site energy for each site in the cell leads to no substantive difference in the density of states.
[6] Charles Kittel, *Introduction to Solid State Physics* (John Wiley & Sons, Inc., New York, 1986), 6th ed., p. 262.
[7] The scattering times in the bulk and metalattice should differ. The interband transitions, nevertheless, are not as sensitive to the scattering time as are the intraband contribution.
[8] H. Ehrenreich, H. R. Philipp, and B. Segall, Phys. Rev. **132**, 1918 (1963).